Advanced high-affinity glycoconjugate ligands of galectins

Michaela Hovorková, Jakub Červený, Ladislav Bumba, Helena Pelantová, Josef Cvačka, Vladimír Křen, Olivier Renaudet, David Goyard, Pavla Bojarová

HAL Id: hal-04294860

https://hal.univ-grenoble-alpes.fr/hal-04294860

Submitted on 20 Nov 2023

Advanced high-affinity glycoconjugate ligands of galectins

Michaela Hovorková [a,b], Jakub Červený [a,c], Ladislav Bumba [a], Helena Pelantová [a], Josef Cvačka [d], Vladimír Křen [a], Olivier Renaudet [e], David Goyard [e,*], Pavla Bojarová [a,f*]

[a] Institute of Microbiology, Czech Academy of Sciences, Vídeňská 1083, CZ-14220 Prague 4, Czech Republic; Phone: (+420) 296442360; Fax: (+420) 244471286; E-mail: bojarova@biomed.cas.cz
[b] Department of Genetics and Microbiology, Faculty of Science, Charles University, Viničná 5, CZ-12843 Prague 2, Czech Republic
[c] Department of Analytical Chemistry, Faculty of Science, Charles University, Hlavova 8, CZ-12843 Prague 2, Czech Republic
[d] Institute of Organic Chemistry and Biochemistry of the Czech Academy of Sciences, Flemingovo nám. 2, CZ-166 10 Prague 6, Czech Republic
[e] Department of Molecular Chemistry, University Grenoble-Alpes, 621 Avenue Centrale, F-38400 Saint Martin-d'Hères, France; E-mail: david.goyard@univ-grenoble-alpes.fr
[f] Department of Health Care Disciplines and Population Protection, Faculty of Biomedical Engineering, Czech Technical University in Prague, CZ-272 01 Kladno, Czech Republic

Abstract: Galectins are proteins of the family of human lectins. By binding terminal galactose units of cell surface glycans, they moderate biological and pathological processes such as cell signaling, cell adhesion, apoptosis, fibrosis, carcinogenesis, and metabolic disorders. The binding of monovalent glycans to galectins is usually relatively weak. Therefore, the presentation of carbohydrate ligands on multivalent scaffolds can efficiently increase and/or discriminate the affinity of the glycoconjugate to different galectins. A library of glycoclusters and glycodendrimers with various structural presentations of the common functionalized *N*-acetyllactosamine ligand was prepared to evaluate how the mode of presentation affects the affinity and selectivity to the two most abundant galectins, galectin-1 (Gal-1) and galectin-3 (Gal-3). In addition, the effect of a one- to two-unit carbohydrate spacer on the affinity of the glycoconjugates was determined. A new design of the biolayer interferometry (BLI) method with specific AVI-tagged constructs was used to determine the affinity to galectins, and compared with the gold-standard method of isothermal titration calorimetry (ITC). This study reveals new routes to low nanomolar glycoconjugate inhibitors of galectins of interest for biomedical research.
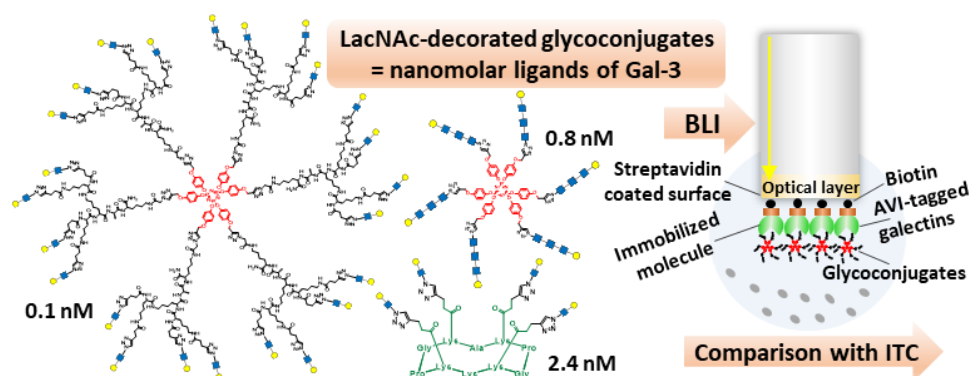
Keywords: biolayer interferometry; carbohydrate; click chemistry; galectin; glycoconjugate; multivalency; transglycosylation.

1. Introduction

Galectins are mammalian lectins that specifically recognize β-galactoside units on cell surfaces [1]. Their carbohydrate recognition domain (CRD) is highly conserved and exhibits sequence similarity throughout the whole family [2]. Through glycan binding, galectins are involved in many physiological processes, such as adhesion, cell migration [3], inter-cellular interactions [4] and signaling [5], apoptosis [6], and pre-mRNA splicing. Galectin-1 (Gal-1) and galectin-3 (Gal-3) are the most abundant and most studied galectins, especially due to their involvement in cancer-related processes. The functions of respective galectins are based on their structural differences. As a bivalent dimer, Gal-1 induces pro-apoptotic factors, which affect T cell survival [7]. Gal-3 has a unique chimeric structure with a C-terminal CRD and an N-terminal tail [8]. It helps tumor cells to escape apoptosis, and supports cell adhesion and migration during metastasis [7]. Therefore, the inhibition of Gal-1 and Gal-3 is a promising approach to cancer treatment.

Typical ligands of galectins are lactose (Galβ4Glc) and *N*-acetyllactosamine (LacNAc; Galβ4GlcNAc). However, the binding of such monovalent unmodified ligands is relatively weak. The affinity to galectins can be increased by modifying the carbohydrate moiety, for example by an aromatic substitution at the C-3 position [9–11]. An even more effective approach to increase the affinity is multivalent presentation that provides a broad spectrum of interactions occurring only in multivalent systems [12]. Galectin-carbohydrate interactions are reinforced by a dense carbohydrate presentation on glycoproteins that can induce high avidity through multivalent effect (*i.e.*, glycocluster effect) [13]. Synthetic glycoconjugates are based on many types of scaffolds, such as polymers [14,15], dendrimers [16–18], calixarenes [19], serum albumins [20,21] or peptides [22,23]. Peptide structures are suitable for the development of therapeutic biomaterials due to their natural origin, biodegradability, and non-inflammatory behavior. Restuccia *et al*. [22] prepared self-assembled glycopeptide nanofibers with LacNAc to substantially increase the affinity to Gal-1. Galectin-binding nanofibers efficiently inhibited the Gal-1-mediated T cell apoptosis [22]. In the follow-up study, they prepared selective inhibitors of Gal-3 based on glycopeptide nanofibers decorated with *N,N´*-diacetyllactosamine that inhibited the pro-apoptotic activity of Gal-3 in Jurkat T cells [23]. In general, glycopeptides and glycodendrimers are strong ligands of many different lectins, and often have a high biomedical potential [24]. For example, glycocluster ligands of LecA and LecB lectins from *Pseudomonas aeruginosa* could effectively bind to the bacterial surface and activate the immune response [25], and mannosylated glycodendrimers acted as anti-adhesive ligands against BC2L-A lectin from *Burkholderia cenocepacia* [26].

In addition to the scaffold structure, the type of the linker between the sugar and the carrier has a significant effect on the affinity to galectins. In previous studies, Elling's group [10,20,27], used a thiourea linker for conjugation of carbohydrate units to serum albumins. In another study, Bojarová *et al*. [14] presented a structure-affinity relationship study with four different spacers and two different carbohydrate functionalities – *O*-ethyltriazole and *N*-triazole. It was found that the direct *N*-triazole linker more efficiently inhibited Gal-3 as the affinity to Gal-3 decreased in the order *N*-triazole > *O*-ethyltriazole > thiourea. Based on these results, we selected the most effective *N*-triazole linker for this study, aimed at the preparation of highly efficient glycocluster inhibitors of galectins.

In this work, a library of seven glycopeptides and glycoclusters with various types of multivalent presentations of the commonly used LacNAc ligand was prepared. The effect of

the type of presentation on the affinity and selectivity to Gal-1 and Gal-3 was thoroughly studied using a new setup of biolayer interferometry (BLI) with specific AVI-tagged constructs of galectins. The results were correlated with the gold-standard method of isothermal titration calorimetry (ITC). To evaluate the influence of the type of carbohydrate spacer, we prepared azido-functionalized chito-LacNAc ligands (LacNAc-$(GlcNAc)_n$-N_3; n = 0-2) and conjugated them to hexavalent cyclotriphosphazene-based scaffold **11**. Thus, we revealed the influence of the spacer length on the affinity of the glycocluster to Gal-1 and Gal-3. The present study, in combination with the existing literature [14,20], gives a detailed picture of the effect of different types of linkers and multivalent structural presentations of galectin ligands, and points a route to nanomolar glycocluster inhibitors of galectins with biomedical potential.

2. Experimental Section

2.1. Biotinylated His₆-tagged Gal-1 containing Avi-tag sequence on a linker (Gal-1-AVI_link)

2.1. Biotinylated His$_6$-tagged Gal-1 containing Avi-tag sequence on a linker (Gal-1-AVI$_{link}$)

For the preparation of His$_6$-tagged Gal-1 construct with AVI-tag sequence on a linker (Gal-1-AVI$_{link}$), we cloned the synthetic DNA string of 474 bp containing His$_6$-tag, AVI-tag, and a peptide linker of 15 amino acids (Invitrogen, Life Technologies, Carlsbad, CA, USA; for details see the Supporting Information, Figure S2) into pETDuet1 vector (restriction sites *Nco*I/*Asc*I) using Gibson assembly technique [28]. For the Gibson assembly, a mixture composed of ISO buffer, T5 exonuclease (5.3 U/mL), Phusion® High-Fidelity DNA polymerase (33 U/mL), Taq DNA ligase (5.3 U/µL), linearized vector (50 µg/ml), and the DNA string (50 µg/mL) was incubated at 50 °C for 1 h. Then, the vector carrying the assembled amended gene of Gal-1-AVI$_{link}$ was used for the transformation of *E. coli* TOP10 for amplification. After isolation of plasmid using Genopure Plasmid Midi Kit (Roche, Basel, Switzerland) and confirmation by sequencing, the construct was recombinantly expressed in *E. coli* BL21(λDE3) cells carrying the *birA* gene for *in vivo* biotinylation as described below.

2.2. Production of galectin constructs

2.2. Production of galectin constructs

The recombinant human galectins Gal-1 and Gal-3 for ITC assays were produced as N-terminal His-tagged constructs cloned in the pET-Duet1 vector (restriction sites *Nco*I/*Asc*I) and purified as described previously [9,27]. Briefly, transformed *E. coli* Rosetta 2(DE3)pLysS competent cells were incubated overnight in LB medium (60 mL) and cultivated at 37 °C and 220 rpm overnight. The precultures were inoculated into Terrific Broth medium (TB; 600 mL; 12 g/L tryptone, 24 g/L yeast extract, 4 mL/L glycerol, 2.31 g/L KH$_2$PO$_4$, 12.54 g/L K$_2$HPO$_4$) and cultivated at 37 °C and 120 rpm. The LB and TB media were supplemented with ampicillin (100 µg/mL) and chloramphenicol (34 µg/mL). Protein expression was induced by adding 0.5 mM IPTG when the culture reached an optical density (OD$_{600}$) of 0.6-0.8. Then, the cells were cultivated at 25 °C for 24 h and harvested by centrifugation (8880 × g, 20 min, 4 °C).

The galectin constructs carrying an AVI-tag (Gal-1-AVI$_{link}$ and Gal-3-AVI [9]) cloned into the vector pET-Duet1 (restriction sites *Nco*I/*Asc*I) were expressed in *E. coli* BL21(λDE3) (Takara Bio, Kusacu, Japan) competent cells as described previously [27]. The *E. coli* strain contained an IPTG-inducible plasmid carrying the gene of biotin ligase *birA* for selective *in vivo* mono-biotinylation of the AVI-tags of galectin constructs. The cells were grown in MDO medium (20 g/L yeast extract, 20 g/L glycerol, 1 g/L KH$_2$PO$_4$, 3 g/L K$_2$HPO$_4$, 2 g/L NH$_4$Cl, 0.5 g/L Na$_2$SO$_4$, 0.01 g/L thiamine hydrochloride) supplemented with ampicillin (150

µg/mL), and chloramphenicol (10 µg/mL) and complemented with 50 µM D-biotin (12 µg/mL) before induction. After induction with 1 mM IPTG at an OD_{600} of 0.6), the cultures were grown for additional 4 h at 37 °C and harvested by centrifugation (8880 × g, 20 min, 4 °C).

For purification of all galectins, harvested cells were sonicated in equilibration buffer (20 mM phosphate/500 mM NaCl/20 mM imidazole, pH 7.4) for cell disruption (1 min pulse, 2 min pause, 6 repetitions). After centrifugation (20 230 × g, 20 min, 4 °C), the cell-free extract was used to load an equilibrated Ni-NTA column (GE Medical Systems, Prague, Czech Republic). First, the loaded column was washed with equilibration buffer, then with equilibration buffer containing 0.5% Triton X100 (10- to 20-fold column volume) to remove lipopolysaccharide [9]. Then the column was washed again with pure equilibration buffer. The protein was eluted with elution buffer containing 500 mM imidazole. Fractions were analyzed for protein content using Bradford assay [29], pooled and dialyzed overnight in PBS buffer (phosphate-buffered saline) pH 7.5 (7 L) containing 2 mM EDTA (ethylenediamine tetraacetic acid) followed by 4 h in PBS buffer (7 L). Gal-3, Gal-1, Gal-1-AVI$_{link,}$ and Gal-3-AVI proteins were stable at 4 °C for approximately two months. The purity of the prepared galectins was confirmed by SDS-PAGE (12% gel; Supporting Information, Figure S1) and the presence of bound biotin was verified by Western blot. In the case of Gal-1 and Gal-3, the usual yield was *ca.* 9 g of cells per 1 L of medium with *ca.* 2 mg of pure galectin per 1 g cells. In the case of the biotinylated AVI-constructs, the usual yield of Gal-1-AVI$_{link}$ and Gal-3-AVI was *ca.* 3 g cells per 1 L medium with *ca.* 1.5 mg pure biotinylated galectin per 1 g cells.

2.3. Synthesis of (2-acetamido-2-deoxy-β-D-glucopyranosyl)$_n$ azide precursors 3, 4

Compounds **3** (2-acetamido-2-deoxy-β-D-glucopyranosyl-(1→4)-2-acetamido-2-deoxy-β-D-glucopyranosyl azide; (GlcNAc)$_2$-N$_3$) and **4** (2-acetamido-2-deoxy-β-D-glucopyranosyl-(1→4)-2-acetamido-2-deoxy-β-D-glucopyranosyl-(1→4)-2-acetamido-2-deoxy-β-D-glucopyranosyl azide; (GlcNAc)$_3$-N$_3$) were synthesized as follows. The glycosyl donor *p*NP-β-GlcNAc (**2**; 50 mM, 205 mg) and the acceptor 2-acetamido-2-deoxy-β-D-glucopyranosyl azide (**1**, GlcNAc-N$_3$, prepared as described previously [30]; 100 mM, 289 mg) were dissolved in 50 mM citrate-phosphate buffer pH 5.0. The Y470N *Tf*Hex (7 mg, 19.2 U, 305 µL) was added (total reaction volume 12 mL) and the reaction mixture was shaken at 35 °C and 1000 rpm. The reaction was monitored by TLC (thin-layer chromatography). After 1.5 h another portion of donor **2** (50 mM, 205 mg) was added. When the donor was consumed (*ca.* after 5.5 h) the reaction was stopped by denaturing the enzyme at 99 °C for 2 min and centrifuged at 12 100 × g for removing the denatured enzyme. The supernatant was purified by gel permeation chromatography (Biogel P2, Bio-Rad Labs., Prague, Czech Republic) at a flow rate of 6.0 mL/h with water as the mobile phase. The fractions containing pure separated products **3** and **4** were pooled and lyophilized. The title compounds **3** and **4** were obtained as white fluffy solids. The isolated yields were 180 mg (33%) of compound **3** and 118 mg (15%) of compound **4**. For structural analysis see the Supporting Information, Table S2, Figure S3a-S3d for compound **3**; Table S3, Figure S4a-S4d for compound **4**.

2.4. Synthesis of β-D-galactopyranosyl-(1→4)-(2-acetamido-2-deoxy-β-D-glucopyranosyl)$_n$ azide ligands (6, 7, 8)

Compound **6** (LacNAc-N$_3$, β-D-galactopyranosyl-(1→4)-2-acetamido-2-deoxy-β-D-glucopyranosyl azide) was synthesized as described previously [31]. Briefly, the glycosyl donor *p*NP-β-Gal (**5**; 30 mM, 36 mg) and the acceptor GlcNAc-N$_3$ (**1**; prepared as described

previously [30]; 150 mM, 148 mg) were suspended in 50 mM sodium phosphate buffer pH 6.0, and β-galactosidase BgaD-A (252 µg, 2.4 U, 260 µL) was added. The reaction was shaken at 35 °C and 850 rpm, and after 2 h another portion of donor **5** (27 mg) was added. The reaction mixture was purified as described in Section 2.7. The title compound **5** was obtained as a white, fluffy solid. The isolated yield was 15 mg (18%) with the BgaD-A-WT. The structural integrity of compound **5** was confirmed by NMR and the data were in agreement with those reported in the literature [15]. The HRMS data for **5** are given in the Supporting Information (Figure S6).

Compounds **7** (β-D-galactopyranosyl-(1→4)-2-acetamido-2-deoxy-β-D-glucopyranosyl-(1→4)-2-acetamido-2-deoxy-β-D-glucopyranosyl azide, LacNAc-GlcNAc-N_3) and **8** (β-D-galactopyranosyl-(1→4)-2-acetamido-2-deoxy-β-D-glucopyranosyl-(1→4)-2-acetamido-2-deoxy-β-D-glucopyranosyl-(1→4)-2-acetamido-2-deoxy-β-D-glucopyranosyl azide, LacNAc-(GlcNAc)$_2$-N_3) were synthesized after optimization at the analytical scale. The reaction mixtures (100 µL) contained donor *p*NP-β-Gal (**5**; 30 mM) and acceptor **3** (90-150 mM) or acceptor **4** (90-150 mM) in 50 mM sodium phosphate buffer pH 5.0 and β-galactosidase from *B. circulans* BgaD-B (0.01-0.5 U/mL). The reactions were incubated at 35 °C and 850 rpm and monitored by TLC and HPLC. The optimized reaction conditions were used for the preparatory synthesis of compounds **7** and **8**.

For the preparatory synthesis of compound **6**, the glycosyl donor *p*NP-β-Gal (**5**; 30 mM, 36 mg) and acceptor **3** (100 mM, 180 mg) were dissolved in 50 mM sodium phosphate buffer pH 5.0 and β-galactosidase BgaD-B (50.4 µg, 0.28 U, 8 µL) was added (total reaction volume 4.0 mL). For the preparative synthesis of compound **7**, the glycosyl donor *p*NP-β-Gal (**5**; 30 mM, 24.3 mg) and acceptor **3** (100 mM, 163 mg) were dissolved in 50 mM sodium phosphate buffer pH 5.0 and β-galactosidase BgaD-B (15.8 µg, 85 mU, 2.5 µL) was added (total reaction volume 4.0 mL). The reactions were incubated at 35 °C and 850 rpm and monitored by TLC. When the donor was consumed (*ca*. after 5-6 h) the reactions were stopped by enzyme denaturation at 99 °C for 2 min and centrifuged at 12,100 × g for removing the denatured enzyme. The supernatants were purified as in Section 2.7. Compounds **7** and **8** were obtained as white fluffy solids. The isolated yields were 32 mg (44%) for **7** and 9 mg (14%) for **8**. For structural analysis see the Supporting Information, Figure S5a-S5b for compound **6**; Table S4, Figure S6a-S6d for compound 7; Table S5, Figure S7a-S7d for compound **8**.

2.5. Synthesis of glycoclusters 12-14, 24 and 25 by CuAAC

A solution of CuSO$_4$·5H$_2$O (0.1 eq. per alkyne), THPTA (tris-hydroxypropyltriazolylmethylamine; 0.2 eq. per alkyne) and sodium ascorbate (1 eq. per alkyne) in PBS buffer (400 µL, pH 7.4) was added to a solution of azido-carbohydrates **6-8** (1.1 eq. per conjugation site) and alkynylated scaffold **9-11** (1 eq.) in 400 µL of a 1:1 mixture of DMF/PBS buffer (1:1; pH 7.4). The mixture was degassed under argon and stirred at room temperature for 2 h. The completion of the reaction was monitored by UPLC-MS (ultra performance liquid chromatography – mass spectrometry). To remove copper, Chelex® resin was added and stirred for additional 45 minutes. The crude mixture was purified by semi-preparative RP-HPLC to afford the desired compound as a white solid after lyophilization.

Glycocluster **12** was prepared according to the General procedure from scaffolds **9** (10.9 mg, 8.13 µmol) and **6** (14.6 mg, 35.75 µmol). The crude mixture was purified using a gradient of 0-30% B and the title compound was obtained as a white solid after lyophilization (yield 15.5 mg, 5.20 µmol, 64%). For structural characterization see the Supporting Information, Figure S10a-S10c.

Glycocluster **13** was prepared according to the general procedure from scaffolds **10** (11.0 mg, 11.94 µmol) and **6** (21.5 mg, 52.54 µmol). The crude mixture was purified using a gradient of 0-20% B and the title compound was obtained as a white solid after lyophilization (yield 18.2 mg, 7.13 µmol, 60%). For structural characterization see the Supporting Information, Figure S11a-S11c.

Glycocluster **14** was prepared according to the general procedure from scaffolds **11** (5.5 mg, 5.40 µmol) and **6** (14.6 mg, 35.75 µmol). The crude mixture was purified using a gradient of 0-50% B and the title compound was obtained as a white solid after lyophilization (yield 15.2 mg, 4.38 mmol, 81%). For structural characterization see the Supporting Information, Figure S12a-S12d.

Glycocluster **24** was prepared according to the general procedure from scaffolds **11** (7.5 mg, 7.37 µmol) and **7** (29.7 mg, 48.64 µmol). The crude mixture was purified using a gradient of 5-50% B and the title compound was obtained as a white solid after lyophilization (yield: 19 mg, 4.05 µmol, 55%). For structural characterization see the Supporting Information, Figure S17a-S17d.

Glycocluster **25** was prepared according to the general procedure from scaffolds **11** (1.4 mg, 1.8 µmol) and **8** (7.4 mg, 9.12 µmol). The crude mixture was purified using a gradient of 5-50% B and the title compound was obtained as a white solid after lyophilization (yield 4.0 mg, 0.68 µmol, 49%). For structural characterization see the Supporting Information, Figure S18a-S18d.

2.6. Synthesis of glycodendrimers *18, 20, 22* and *23* by copper-catalyzed azide-alkyne cycloaddition (CuAAC)

A solution of $CuSO_4 \cdot 5H_2O$ (0.1 eq. per alkyne), THPTA (0.2 eq. per alkyne) and sodium ascorbate (1 eq. per alkyne) in PBS buffer (400 µL, pH 7.4) was added to a solution of scaffold **11**, **17**, **19** or **21** (1 eq.) and functionalized polylysine-based dendron **15** or **16** (1.1 eq. per conjugation site) in 400 µL of a mixture of DMF/PBS buffer (1:1; pH 7.4). The mixture was degassed under argon and stirred at room temperature for 2 h. The completion of the reaction was monitored by UPLC-MS. To remove copper, Chelex® resin was added and stirred for additional 45 minutes. The crude mixture was purified by semi-preparative RP-HPLC to afford the desired glycodendrimers.

Glycodendrimer **18** was prepared according to the general procedure from scaffold **17** (2.1 mg, 1.90 µmol) and dendron **15** (22 mg, 8.35 µmol). The crude mixture was purified using a gradient of 5-20% B and the title compound was obtained as a white solid after lyophilization (yield 11.1 mg, 0.95 µmol, 50%). For structural characterization see the Supporting Information, Figure S13a-S13c.

Glycodendrimer **20** was prepared according to the general procedure from scaffold **19** (2.0 mg, 2.48 µmol) and dendron **15** (28.0 mg, 10.89 µmol). The crude mixture was purified using a gradient of 5-30% B and the title compound was obtained as a white solid after lyophilization (yield 15.5 mg, 1.36 µmol, 55%). For structural characterization see the Supporting Information, Figure S14a-S14c.

Glycodendrimer **22** was prepared according to the general procedure from scaffold **21** (3.2 mg, 1.72 µmol) and dendron **15** (30.0 mg, 11.39 µmol). The crude mixture was purified using a gradient of 5-30% B and the title compound was obtained as a white solid after lyophilization (yield 14.1 mg, 1.14 µmol, 66%). For structural characterization see the Supporting Information, Figure S15a-S15c.

Glycodendrimer **23** was prepared according to the general procedure from scaffold **11** (0.9 mg, 0.94 µmol) and dendron **16** (16.4 mg, 6.22 µmol). The crude mixture was purified using a gradient of 5-40% B and the title compound was obtained as a white solid after lyophilization (yield 12.5 mg, 0.75 µmol, 79%). For structural characterization see the Supporting Information, Figure S16a-S16d.

2.7. Determination of the affinity of prepared glycoclusters to galectins by BLI

The affinity and kinetics of prepared glycoclusters were assessed by biolayer interferometry (BLI). The measurements were performed at 25 °C with continuous shaking at 850 rpm using OctetRed96e BLI device (ForteBio, Fremont, CA, USA). For this experiment, *in vivo*-biotinylated galectin constructs (Gal-1-AVI$_{link}$ or Gal-3-AVI) were immobilized on the BLI tips *via* biotin-streptavidin binding. AVI-tagged galectins were diluted to a final concentration of 1 µg/mL in PBS buffer supplemented with 0.05% Tween-20 (PBS-T) and for 180 s they were incubated with streptavidin biosensor tips (Octet® SA Biosensors ForteBio, Fremont, CA, USA) pre-equilibrated in PBS-T for 600 s. The coupling concentration of AVI-tagged galectins was selected to minimize non-specific binding and mass transfer effect. After protein loading, the tips were washed with PBS-T (300 s), immersed into serially diluted solutions of glycoclusters (0.1 nM – 40 µM) in PBS-T, and their association (450 s) and dissociation phases (450 s) were monitored. The obtained data were analyzed by Octet Analysis software (ForteBio, Fremont, CA, USA). For the resulting sensograms, the background interaction of the reference ligand and ligand nonspecific interaction were subtracted. The equilibrium dissociation constant K_D was obtained by nonlinear least-square analysis of the response wavelength shifts in the steady-state regions plotted as a function of the glycoconjugate concentration using Equation 1:

$$R_{eq} = R_{max} \frac{c}{K_D + c} \qquad (1)$$

where R_{eq} is the value of the response shift in the steady-state region in each sensorgram curve, R_{max} is the maximal response in the steady-state region and c is the concentration of glycocluster. This kinetic model is used in the case of complex systems or matrices, or when there is rapid saturation and rapid wash-out of the analyte, such as in our case. This analysis tends to be more time-consuming than other kinetic models due to the need to reach the steady state of the system. After equilibrium was reached, the equilibrium dissociation constant K_D was determined, which describes the system only at equilibrium, not its dynamic side. To make the results for all glycoclusters comparable, the steady-state analysis was used throughout the whole set. Three scaffolds with no carbohydrate attached (**9**, **10** and **11**) were measured as negative controls by the same method (Supporting Information, Figure S19).

Furthermore, to exclude potential cooperativity in our BLI data, we performed nonlinear regression analysis of the response wavelength shifts using Hill Equation 2:

$$R_{eq} = R_{max} \frac{c^H}{K_D{}^H + c^H} \qquad (2)$$

where H corresponds to a Hill coefficient.

2.8. Determination of the affinity of prepared glycoclusters to galectins by ITC

Isothermal titration calorimetry (ITC) experiments were performed with a PEAQ-ITC isothermal titration calorimeter (Malvern Instruments, Malvern UK) at 25 °C. Lyophilized glycoclusters and Gal-1 or -3 were dissolved in the same PBS buffer. Galectins (40-75 µM;

monomer concentration) were placed in the 200 μL sample cell operating at 25 °C. In the frame of optimization of the experimental setup and to verify the correctness and reproducibility of acquired K_D values, three different galectin concentrations (20–150 μM, monomer concentration) were assayed with representative glycocluster **14**, with the same resulting K_D values (Supporting Information, Figure S33). The stoichiometry values reported herein are always related to monomer concentration, *i.e.*, the concentration of lectin binding sites. Titrations were performed with 20 injections of monovalent compounds LacNAc, **6**, **7**, and **8** (0.5-2 mM) or glycoconjugates (15 μM - 2 mM, 2 μL) spaced by 150 s. The experimental data were fitted to a theoretical titration curve using the supplied MicroCal PEAQ-ITC analysis software with ΔH (enthalpy change), K_D (equilibrium dissociation constant), and n (number of ligand molecules per lectin monomer at the equilibrium; the inflection point of the titration curve) as adjustable parameters. In the case of monovalent ligands LacNAc, and **6**-**8**, given the shape of the curve and the excess of ligand necessary to obtain a reliable K_D, stoichiometry at the equilibrium could not be determined accurately; therefore, we decided not to report n values there. Free energy change (ΔG) and entropy contributions ($T\Delta S$) were derived from Equation 2:

$$\Delta G = \Delta H - T\Delta S = -RT\ln K_a \tag{3}$$

where T is the absolute temperature, $R = 8.314$ J/mol/K and $K_a = 1/K_D$. Two independent titrations were performed for each tested ligand. Three scaffolds with no carbohydrate attached (**9**, **10** and **11**) and free GlcNAc were measured as negative controls by the same method (Supporting Information, Figures S22-S25). Preparation of negative control glycodendrimers carrying only GlcNAc by, e.g., β-galactosidase treatment, was technically not feasible due to low amounts of prepared conjugates (several miligrams). Similarly, from our experience, selective synthesis of heterogenous but well-defined conjugates (i.e., carrying only one LacNAc with other sites unreacted or occupied with GlcNAc), to possibly further study the multivalent effect, is experimentally extremely challenging, and may form a separate project in the future.

3. Results

3.1. Chemo-enzymatic synthesis of azido-functionalized carbohydrate ligands

The synthesis of ligand **6** (LacNAc-N$_3$) was essentially performed as described previously [31]. For the galactosylation reaction, *p*NP-β-Gal (**2**) was used as a glycosyl donor and GlcNAc-N$_3$ (**1**) as an acceptor. The enzymatic synthesis was catalyzed by β-galactosidase from *B. circulans* [31] and afforded **6** in 15% yield. Alternatively, the same reaction with the synthetically potent mutant E532G BgaD-A afforded a higher yield of **6** (44%) [31].

The first step for the preparation of ligands LacNAc-GlcNAc-N$_3$ (**7**) and LacNAc-(GlcNAc)$_2$-N$_3$ (**8**) containing the chitooligomer spacers was the synthesis of the respective precursors (GlcNAc)$_2$-N$_3$ (**3**) and (GlcNAc)$_2$-N$_3$ (**4**) as shown in Scheme 1. These compounds were synthesized in one pot in a single-step transglycosylation reaction under the catalysis by mutant Y470N β-*N*-acetylhexosaminidase from *T. flavus* (Y470N *Tf*Hex), which has a high synthetic potential for longer oligosaccharides chains. The enzyme Y470N *Tf*Hex was expressed extracellularly in *P. pastoris* and was easily purified in one step by cation-exchange chromatography at pH 3.5 [32,33]. For the transglycosylation reaction, *p*NP-GlcNAc (**2**) was used as a glycosyl donor and GlcNAc-N$_3$ (**1**) as an acceptor. The reaction mixture containing

both products **3** and **4** was purified by gel permeation chromatography to afford pure compounds **3** and **4** at a scale of several hundreds of milligrams.

For the synthesis of galactosyl-capped compounds **7** and **8**, we used the truncated isoform B of β-galactosidase from *B. circulans* (BgaD-B), which showed better performance (yield and selectivity) in analytical reactions than BgaD-A. The preparation of the gene, the production of BgaD-B in *E. coli* and purification by affinity chromatography on HisTrap™ column were performed as described previously [34]. In the preparative galactosylation reaction, the chito-spacers **3** or **4** were used as acceptors and compound **5** (*p*NP-β-Gal) as a glycosyl donor under the formation of azido-functionalized galectin ligands **7** and **8**, respectively (Scheme 1), in sufficient yields for conjugation.
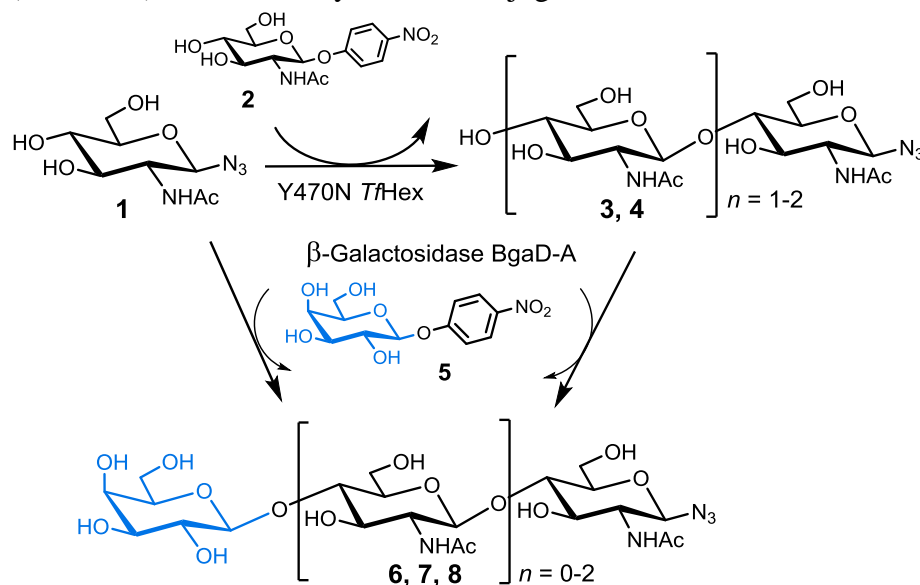
Scheme 1. Chemo-enzymatic synthesis of chitooligomer spacers **3** (*n* = 1), and **4** (*n* = 2) and of ligands **6** (*n* = 0), **7** (*n* = 1), and **8** (*n* = 2).

3.2. Preparation of a library of glycoclusters

Tetra- and hexavalent glycoclusters **12**-**14** were synthesized *via* copper-catalyzed azide alkyne cycloaddition (CuAAC) between polyalkynylated scaffolds **9**-**11** and azido-functionalized *N*-acetyllactosamine **6** (Scheme 2). The respective alkyne-containing carriers cyclodecapeptide **9** and polylysine dendron **10** were prepared by adapting previously reported procedures [35,36]. Cyclotriphosphazene-based carrier **11** was prepared in one step by nucleophilic substitution of *p*-propargyl phenol on the commercial hexachloro-derivative [37].
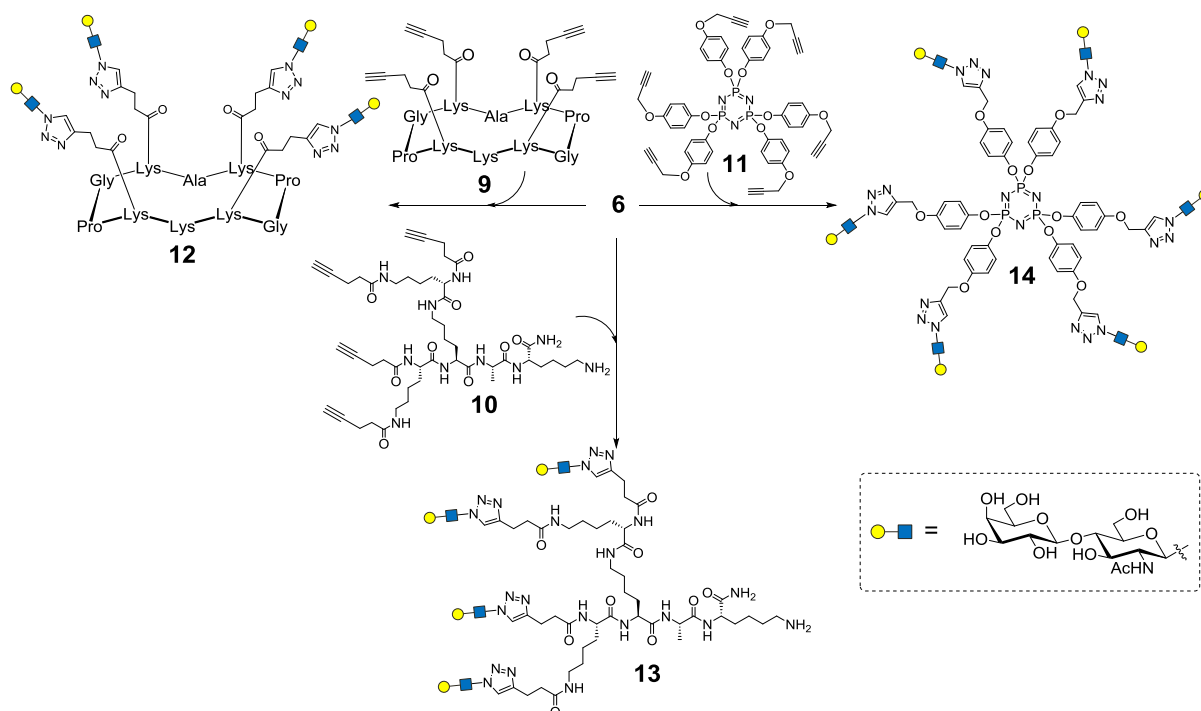
Scheme 2. Multivalent scaffolds **9**, **10**, and **11**, and the resulting LacNAc-decorated first-generation glycoclusters **12**, **13**, and **14**. The Symbol Nomenclature for Glycans (SNFG) was used to abbreviate the monosaccharide units.

After preparing the first-generation glycoclusters **12-14**, a series of second-generation glycodendrons was prepared through a convergent strategy using compound **13** as the glycosylated dendron unit (Scheme 3). The remaining free lysine of **13** was functionalized using *N*-succinimide-activated esters of pentynoic or azidoacetic acid [26] yielding dendrons **15** and **16** respectively. Alkyne-bearing module **15** was coupled with tetraazidated scaffolds **17**, **19** and **21** *via* CuAAC to obtain hexadecavalent glycodendrimers **18** and **20** and tetracosavalent glycodendrimer **22**. Azido-functionalized dendron **16** was reacted with carrier **11** to obtain 24-valent dendrimer **23**. All reactions proceeded with good yields (stated in the Experimental Section) and final compounds **18**, **20**, **22**, and **23** were characterized by NMR, HPLC and HRMS (see the Supporting Information).
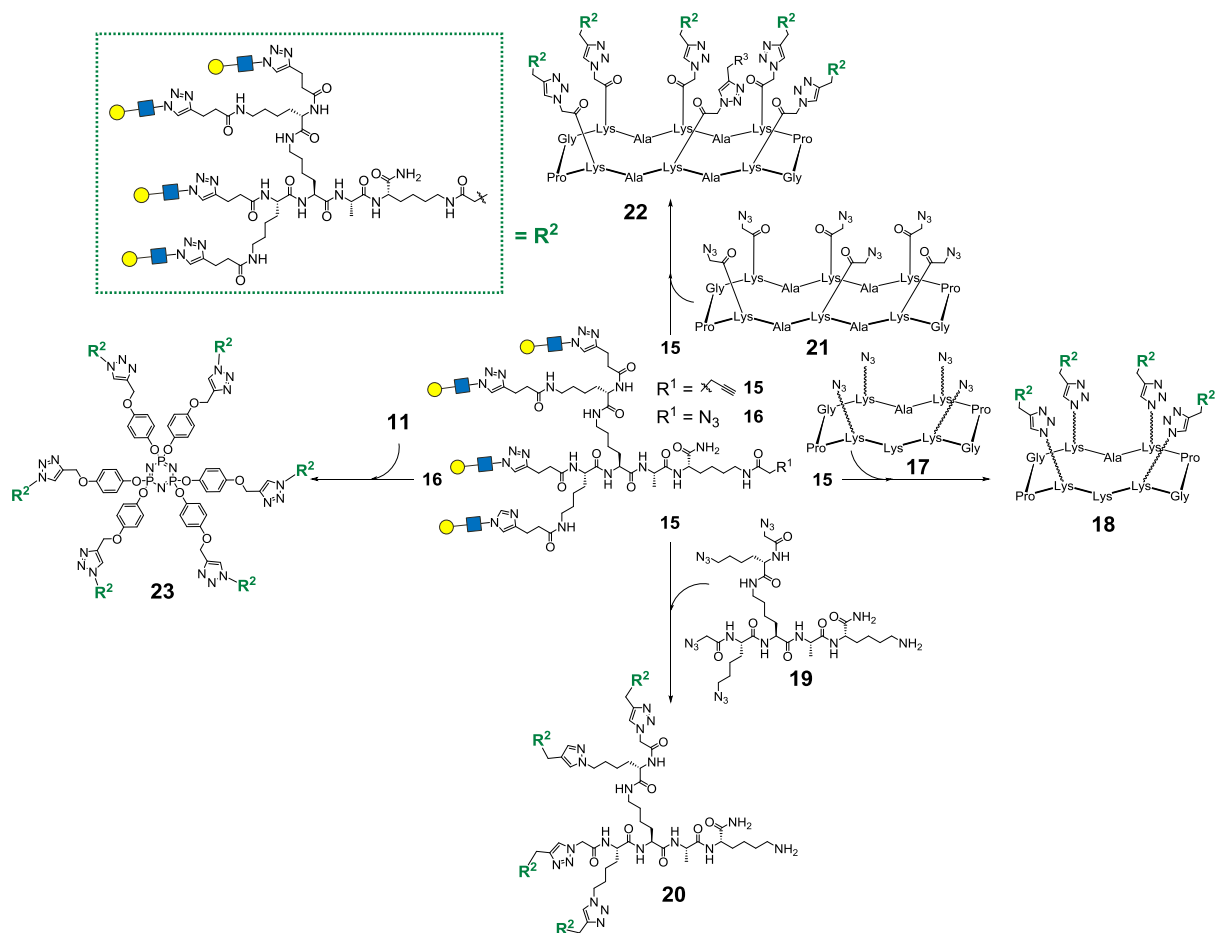
Scheme 3. Synthesis of hexadeca- and tetracosavalent LacNAc glycodendrimers **18**, **20**, **22**, and **23** of the second generation. The Symbol Nomenclature for Glycans (SNFG) was used to abbreviate the monosaccharide units.

The first series of ITC experiments (see Section 3.4.) revealed that cyclotriphosphazene-based glycodendrimer **14** was the most potent ligand of both Gal-1 and -3. Therefore, this carrier was chosen for studying the impact of the presence of the chitooligomer spacer on the affinity to galectins. Carrier **14** was conjugated with chitooligomer-containing ligands LacNAc-GlcNAc-N$_3$ (**7**) or LacNAc-(GlcNAc)$_2$-N$_3$ (**8**) to afford hexavalent clusters **24** and **25** (Figure 1).
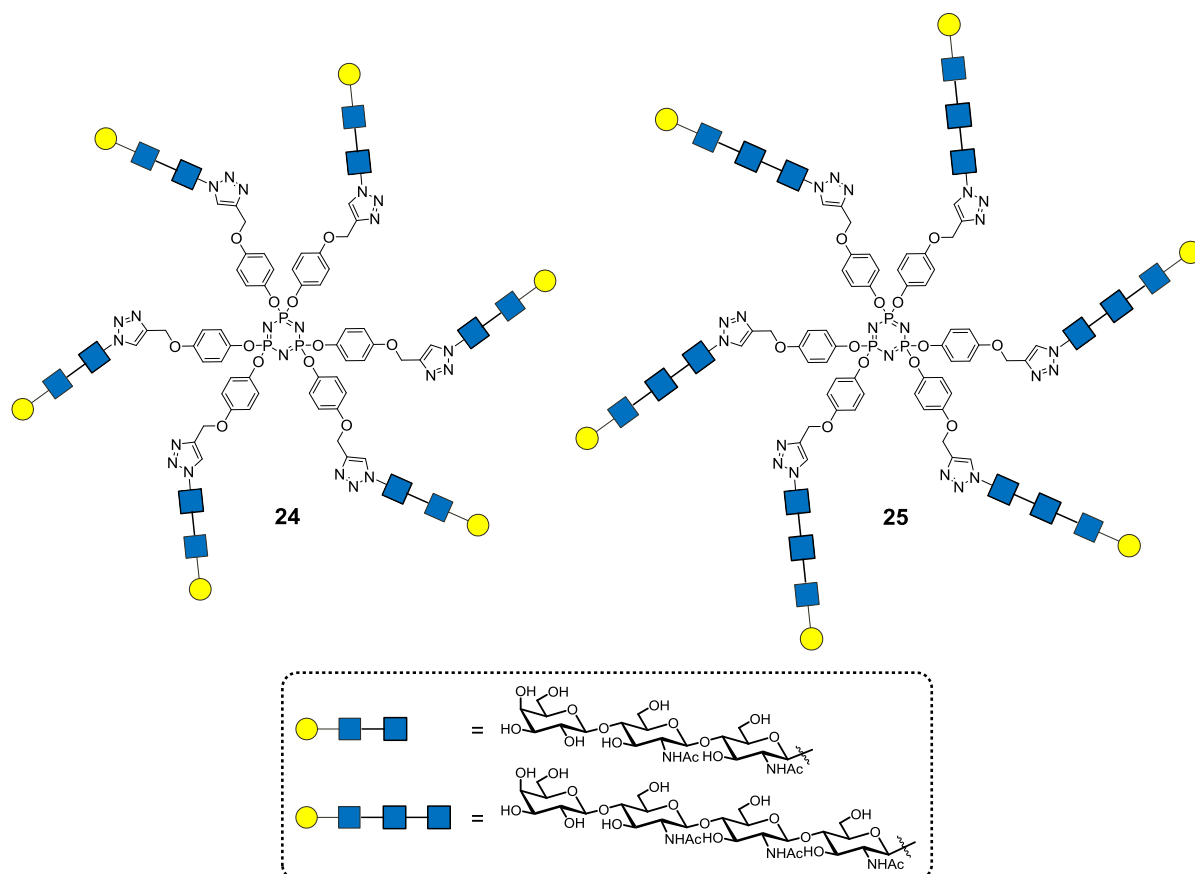
Figure 1. Hexavalent glycoclusters **24** and **25** decorated with LacNAc ligand on one-unit or two-unit chitooligomer spacers. The Symbol Nomenclature for Glycans (SNFG) was used to abbreviate the monosaccharide units.

3.3. Preparation of galectin constructs for analytical measurements

The Gal-1 and Gal-3 proteins were produced in *E. coli* Rosetta 2(DE3)pLysS and purified as described previously [9,27]. For BLI measurements that required galectin immobilization, we used AVI-tagged galectin constructs. They were expressed in *E. coli* BL21(λDE3) cells in the presence of the BirA biotin ligase, which enables *in vivo* biotinylation of the specific lysine residue within the AVI-tag sequence (GLNDIFEAQ**K**IEWHE). Initial BLI experiments showed that in contrast to Gal-3-AVI, which preserved its lectin activity after immobilization, the immobilized AVI-tagged Gal-1 constructs (either at N- or C-terminus) [9] were incapable of binding their carbohydrate ligands. This was most likely due to the close proximity of binding of the Gal-1 molecule to the surface of the biosensor, which prevents glycan recognition due to steric constraints. To overcome this effect, we designed a new construct, Gal-1-AVI$_{link}$, in which the AVI-tag was separated from the protein with a neutral peptide linker (GGSGGSGGSGGSGGS) (Figure 2). The lectin activity of the Gal-1-AVI$_{link}$ construct was verified by ELISA (enzyme-linked immunosorbent assay) and matched the respective unlabeled control (Supporting Information, Table S1).
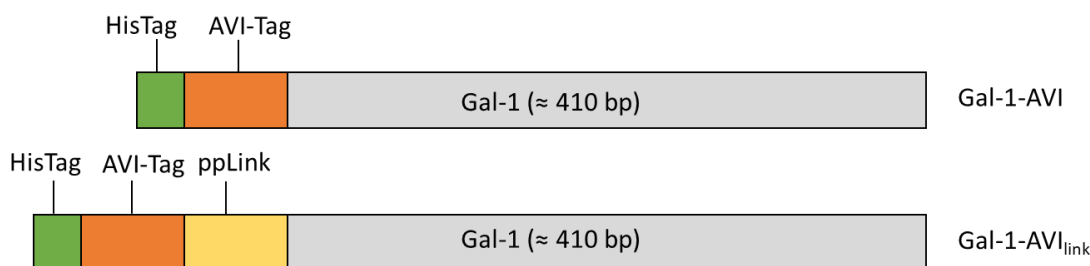
Figure 2. N-terminal Gal-1-AVI and Gal-1-AVI$_{link}$ constructs

3.4. Affinities of prepared glycoconjugates to Gal-1 and Gal-3 determined by BLI

All three structural types of glycoconjugates, based on the cyclotriphosphazene- (**14**, **23**, **24**, **25**), cyclopeptide- (**12**, **18**, **22**), and branched-type- (**13**, **20**) scaffolds, decorated with different amounts of presented LacNAc epitopes (*i.e.*, different valences; Table 1) were investigated using BLI. The experimental set-up of BLI does not allow to measure small-molecule ligands, and therefore it was not possible to measure the affinity of the monovalent LacNAc and negative control GlcNAc. Three representative scaffolds (**9**, **10** and **11**) were used as negative controls and were found not to interact with either galectin or the biosensor (Supporting Information, Figure S19). For the BLI measurement, as for other on-surface measurements such as surface plasmon resonance [27,38], the density of the protein molecules immobilized on the biosensor was optimized in order to prevent diffusion-limited effects known as a mass transfer effect. Thus, the protein molecules (Gal-1-AVI or Gal-3-AVI) were immobilized on the biosensor in the lowest possible density that was sufficient to obtain the signal (R_{max}), but did not enable multiple interactions of a single glycoconjugate with two or more protein molecules immobilized on the biosensor. This corresponds to no cooperativity as reflected on Hill coefficients ranging around 1 (specifically, 0.8-1.2) for all data curves. In the studied series of glycoconjugates, we found that whereas the K_D values for Gal-1 were in the low micromolar to the high nanomolar range, the affinities for Gal-3 were stronger by *ca.* 3-orders of magnitude, *i.e.*, in the low nanomolar to the high picomolar range. Interactions of carbohydrate ligands with lectins in the affinities of picomolar-range are rather rare and with Gal-3 they have so far been observed only with complex oligosaccharide ligands presented on considerably larger-sized neo-glycoproteins (MWs over 70 kDa) using surface plasmon resonance [27]. This large difference in binding between the two galectins is clearly visible in the sensogram curves (Supporting Information, Figure S20, S21). For Gal-1, fast association and dissociation rates were observed. The formation of the complex [L-A] was very fast, leading to a fast equilibrium (steady state) but, upon disturbance, the formed complexes decayed very rapidly. In contrast, for Gal-3, a significant baseline drift was observed during the dissociation phase of the interaction, indicating a prolonged dissociation. In glycoclusters **24** and **25**, the dissociation phase appeared to be more complex, possibly including other interaction phenomena (Supporting Information, Figure S21). Based on these observations, the data obtained were evaluated by the steady-state analysis method (Figure 3).

Common affinity trends were observed throughout the glycoconjugate series with both galectins. The first-generation glycoconjugates (glycoclusters) **12**-**14** with lower valences (4-6 LacNAc) generally exhibited significantly lower binding affinities than the second-generation glycoconjugates (glycodendrimers) **18**, **20**, **22**, and **23** with high valences (16 and 24). From the glycoclusters series, cyclotriphosphazene-based glycocluster **14** was the best binder to both Gal-1 and Gal-3. In the series of second-generation glycodendrimers, virtually no

differences were observed when increasing the valence from 16 to 24 LacNAc with either Gal-1 or Gal-3. This indicates saturation of binding in both cases. The best ligands of the entire series were glycodendrimer **18** for Gal-1 (K_D = 248 nM) and **23** for Gal-3 (K_D = 0.13 nM) but without outstanding lead over the other high-valence glycoclusters. These glycoconjugates were also among those exhibiting the highest multivalent effect for respective galectins, expressed as the highest affinity per one glycan (Supporting Information, Table S6).

The best-performing low-valent glycocluster **14** was selected to compare the effect of the LacNAc presentation on the chitooligomer spacer (ligands **7** and **8**) on the affinity to galectins. When comparing parent glycocluster **14**, glycocluster **24** (one-unit chito-spacer) and **25** (two-units chito-spacer) in binding to Gal-1, a slight improvement in affinity was observed, which corroborates our hypothesis that the nature-like carbohydrate spacer is beneficial for ligand recognition. This was not the case of Gal-3 where the presence of a chito-spacer in glycoconjugates **24** and **25** did not bring a clear positive effect or rather a deterioration of the affinity. This may be due to the fact that the presence of the triazole moiety directly adjacent to the C-1 of LacNAc has non-specific interaction with the E-subsite of the Gal-3 binding groove as also observed previously [14]. Indeed, hexavalent clusters **24** and **25** showed very similar affinities to Gal-3 like compound **14** displaying only LacNAc as an epitope.
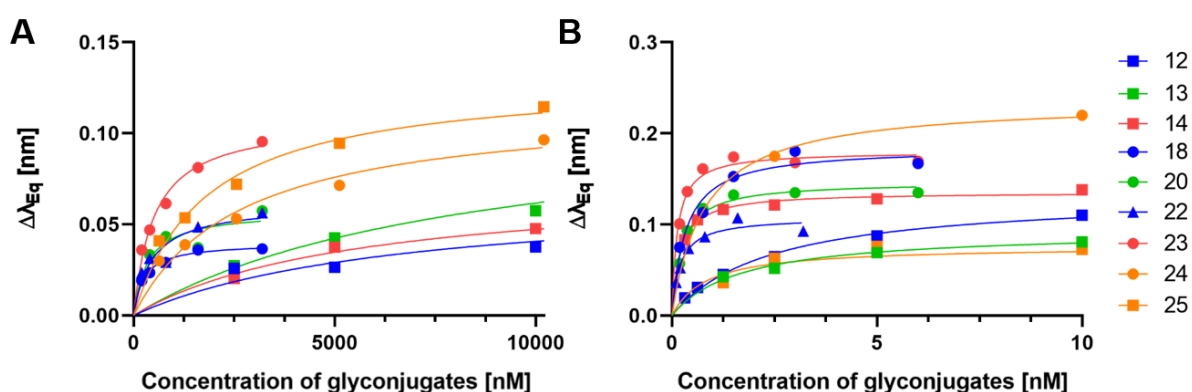

Figure 3. Steady-state analysis of the interaction between galectins and glycocluster by BLI **A.** Interaction with Gal-1-AVI$_{link}$ showing the highest affinities to **22** (K_D = 459 ± 174 nM; valence 24), **20** (K_D = 347 ± 138 nM; valence 16), and especially to **18** (K_D = 248 ± 39 nM; valence 16); **B.** Interaction with Gal-3-AVI showing the highest affinities to **14** (K_D = 0.20 ± 0.02 nM; valence 6), **22** (K_D = 0.19 ± 0.04 nM; valence 24), and especially **23** (K_D = 0.13 ± 0.02 nM; valence 24).

Table 1. Interaction between glycoclusters and galectins assessed by BLI

Compound	Mw	Valence	K_D [nM] Gal-1	Gal-3	Binding mode	Selectivity for Gal-3[b]
12	2990	4	6636 ± 1 382	2.4 ± 0.1	SS[a]	2765
13	2554	4	8389 ± 1 118	1.7 ± 0.2	SS[a]	4935
14	3468	6	5620 ± 514	0.20 ± 0.02	SS[a]	28 100
18	11663	16	248 ± 39	0.33 ± 0.06	SS[a]	752
20	11357	16	347 ± 138	0.23 ± 0.03	SS[a]	1509
22	17668	24	459 ± 174	0.19 ± 0.04	SS[a]	2416
23	16843	24	503 ± 92	0.13 ± 0.02	SS[a]	3869

| 24 | 4687 | 6 | 2659 ± 563 | 0.79 ± 0.14 | SS[a] | 3366 |
| 25 | 5906 | 6 | 1805 ± 251 | 0.84 ± 0.42 | SS[a] | 2256 |

[a] SS, steady-state analysis was performed by the non-linear least-square fitting of the response wavelength shifts in the steady state of the galectin-ligand system

[b] Selectivity for Gal-3 was calculated as the ratio of K_D(Gal-1)/K_D(Gal-3).

3.5. Affinities of prepared glycoconjugates to Gal-1 and Gal-3 determined by ITC

The binding parameters (stoichiometry and thermodynamics) of all prepared glycoclusters and glycodendrimers to Gal-1 (Table 2) and Gal-3 (Table 3) were assayed by ITC (Supporting Information, Figures S22-S39). Monovalent *N*-acetyllactosamine (LacNAc) was used as a reference to determine the relative potency of each compound. For Gal-3, free LacNAc had the same affinity as the azido-functionalized LacNAc-N$_3$ (**6**); for Gal-1, its K_D fell within the values for monovalent LacNAc derivatives **6-8** (40-131 μM). This comparison clearly shows that the influence of the C-1 azido moiety is not significant. The rather large experimental error in some cases is given by the generally low affinities of monovalent ligands and by the necessity of using the excess of ligand.

Three representative scaffolds (**9**, **10** and **11**) were used as negative controls and were found not to interact with either galectin (Supporting Information, Figures S22-S24). Additionally, free GlcNAc was used as a negative control in ITC (due to its small size it could not be measured by BLI) and it was found not to interact with either galectin (Figure S25), which is in full agreement with the literature stating that galectin ligands are galactose-terminated carbohydrates [39–41].

Titrations were performed in the direct injection mode (galectin in the sample cell and ligand in the syringe). The analysis of thermodynamic contributions showed that for all multivalent glycoconjugates, the binding was enthalpy-driven but it was counter-balanced with a strong entropic cost, most likely due to the loss of flexibility induced upon lectin binding. Stoichiometries indicated that most glycoconjugate epitopes participated in the binding with multiple lectin monomers in an aggregative manner, consistent with the relative size of the proteins compared to that of the ligands. Although Gal-1 was most likely present as a homodimer under the used experimental conditions (dimer concentration 20-38 μM) [42,43], the two carbohydrate-binding sites of Gal-1 are located too far apart to be chelated with a single glycoconjugate molecule. The shape of the ITC curves and the general behavior of the system during the measurement indicated that no aggregation processes occured along with the ligand binding, and that both lectins maintained the same aggregation state during the whole experiment in the used range of concentrations – probably homodimer for Gal-1, and monomer for Gal-3 (though oligomerization of Gal-3 was often observed in the literature [44]). To verify the reliability of acquired K_D values, we repeated the measurement of representative glycocluster **14** with different concentrations of galectins (20–150 μM, monomer concentration; Supporting Information, Figure S33). Lower galectin concentrations were unfeasible due to an insufficiently low signal intensity (below 1-2 μW), causing an improper signal/noise ratio. This range of concentrations also agrees well with the previously published experimental setups for galectins by other groups [45,46]. Similar K_D values were obtained for all sets of conditions (for details see legend to Figure S33). Despite the fact that both galectins have comparable affinities for LacNAc-N$_3$ (K_D = 40.2 μM for Gal-1 and 38.3 μM for Gal-3), binding was stronger for Gal-3 with 10 to 20-fold lower K_D values for all glycoconjugates (Tables 2, 3). The improved binding to Gal-3 was in accord with the findings from the BLI method where, however, the observed differences exceeded three orders of

magnitude. Nevertheless, the observed trends were very similar. Among the three LacNAc glycoclusters **12**-**14** of the first generation, cyclotriphosphazene-based compound **14** was the most potent ligand of both galectins, both in terms of K_D and relative potency per LacNAc residue (see also Table S7 in the Supporting Information). This result was in agreement with BLI. When this carrier was used for evaluating the affinity of tri- and tetrasaccharides **7** and **8** carrying the nature-like chitooligomer spacers, ITC showed that the introduction of chitooligomer spacers brought no significant change in binding to Gal-1 since hexavalent compounds **24** and **25** displayed affinities comparable with that of molecule **14**. In the case of Gal-3, the introduction of the chitooligomer spacer at C-1 of the LacNAc ligand brought no effect or rather a slight deterioration of the binding affinity. These results also compared well with that of BLI.

Table 2. Affinities of glycoclusters **12**-**25** to Gal-1 determined by ITC.[a]

Cmpnd	Valence	K_D [nM]	n	-ΔH [kJ/mol]	-ΔG [kJ/mol]	-TΔS [kJ/mol]	α	β
LacNAc	1	99 600 ± 18 400	n.d.	91.1 ± 11	22.9	68.3	–	–
6	1	40 200 ± 15 800	n.d.	21.2 ± 6	25.3	71.0	–	–
7	1	74 800 ± 6150	n.d.	8.12 ± 0.7	23.6	15.5	–	–
8	1	131 000 ± 2000	n.d.	59.5 ± 0.3	22.2	37.4	–	–
12	4	5240 ± 360	0.2	38 ± 2	30.2	7.9	19 *(7.7)*	4.8 *(1.9)*
13	4	4940 ± 360	0.2	55.8 ± 0.2	30.4	25.5	20 *(8.1)*	5.0 *(2.0)*
14	6	1810 ± 410	0.12	87 ± 4	32.9	54.6	55 *(22)*	9.2 *(3.7)*
18	16	233 ± 4	0.030	316 ± 15	37.9	278	428 *(172)*	27 *(11)*
20	16	230 ± 23	0.031	286 ± 11	38.0	248	433 *(174)*	27 *(11)*
22	24	72 ± 7	0.034	270 ± 14	40.9	229	1383 *(563)*	58 *(23)*
23	24	134 ± 23	0.024	450 ± 7	39.3	411	743 *(300)*	31 *(13)*
24	6	1540 ± 250	0.10	87 ± 4	33.2	53.6	27 *(49)*	4.5 *(8.2)*
25	6	1970 ± 390	0.15	38.7 ± 0.3	32.7	59.9	21 *(38)*	3.5 *(6.3)*

[a] Thermodynamic data refer to the moles of ligand, and stoichiometry is expressed as the number of ligand molecules per lectin monomer. Standard deviations are calculated from experimentally derived values (at least two independent experiments). *n* is the number of ligand molecules per lectin monomer at the equilibrium. n.d., not determined. Factor α is the relative potency compared with the monovalent standard LacNAc. Factor β is the relative potency per LacNAc residue. For factors α and β, the values in parentheses are the factors corresponding to their respective monovalent reference glycans **6**, **7** or **8**.

Table 3. Affinities of glycoclusters **12**-**25** to Gal-3 determined by ITC.[a]

Cmpnd	Valence	K_D [nM]	n	-ΔH [kJ/mol]	-ΔG [kJ/mol]	-TΔS [kJ/mol]	α	β
LacNAc	1	38 300 ± 22 500	n.d.	29.1 ± 4.4	25.75	2.9	–	–
6	1	38 300 ± 4150	n.d.	77.8 ± 2.9	25.25	52.55	–	–
7	1	82 700 ± 12 950	n.d.	35.45 ± 8.9	23.35	12.13	–	–
8	1	31 100 ± 1250	n.d.	31.7 ± 0.3	25.8	5.97	–	–
12	4	225 ± 8	0.060	129 ± 7	38.0	91.1	170 *(170)*	43 *(43)*
13	4	392 ± 65	0.072	261 ± 15	36.0	225	98 *(98)*	24 *(24)*
14	6	76 ± 9	0.073	334 ± 1	40.7	293.5	504 *(504)*	84 *(84)*
18	16	86 ± 8	0.045	451 ± 19	40.4	410.5	445 *(445)*	28 *(28)*
20	16	171 ± 34	0.048	540 ± 34	38.7	501.5	224 *(224)*	14 *(14)*
22	24	165 ± 16	0.048	446 ± 8	38.8	408	232 *(232)*	9.7 *(9.7)*
23	24	57 ± 4	0.02	1030 ± 44	41.4	992.5	672 *(672)*	28 *(28)*
24	6	130 ± 9	0.049	309 ± 16	39.4	269	295 *(635)*	49 *(106)*
25	6	96 ± 5	0.07	248 ± 15	40.1	208	400 *(325)*	67 *(66)*

[a] Thermodynamic data refer to the moles of ligand and stoichiometry is expressed as the number of ligand molecules per lectin monomer. Standard deviations are calculated from experimentally derived values (at least two independent experiments). *n* is the number of ligand molecules per lectin monomer at the equilibrium. n.d.,

not determined. Factor α is the relative potency compared with the monovalent standard LacNAc. Factor β is the relative potency per LacNAc residue. For factors α and β, the values in parentheses are the factors corresponding to their respective monovalent reference glycans **6**, **7** or **8**.

In the case of glycodendrimers **18**, **20**, **22**, and **23** with higher valences, the observed differences in affinity between the two galectins were not substantial and the K_D values were in the same range (K_D between 57 and 233 nM). Nevertheless, in the case of Gal-1, the multivalent effect increased with the valence. For example, the relative potency per LacNAc residue for glycodendrimer **22**, the most potent ligand ($K_D = 72$ nM), was significantly higher than for glycocluster **14** with a β-factor of 58 versus 9.2 related to LacNAc, respectively. However, in the case of Gal-3, no significant improvement was found in 16- and 24-valent compounds, which had lower β-factors than tetra- and hexavalent clusters **12**-**14**. Compound **23**, the most potent glycocluster (valence 24), had a similar affinity to glycocluster **14** (valence 6), *cf.* $K_D = 57$ nM and 76 nM, respectively, which confirms the lack of significant enhancement brought by higher-valence compounds. These trends are also clearly visible on K_D values recalculated per LacNAc residue (Table S7 in the Supporting Information) and are consistent with previous observations on various scaffolds that involved the saturation of binding between Gal-3 and multivalent ligands [10,14,20,27], and also with BLI.

4. Discussion

The present work shows a promising potential of high-molecular-weight multivalent glycoconjugates for binding galectins, especially the most-studied cancer-related Gal-3. It demonstrates the influence of the LacNAc valence, scaffold topology and structure of the spacer in the close vicinity to the LacNAc epitope. A novel biolayer interferometry design was introduced that enables a fast assessment of binding parameters such as K_D, using selectively mono-biotinylated AVI-tagged galectin constructs. The applicability of this method has thus been demonstrated with two structural types of galectins – the previously studied chimera-type Gal-3 and now with the non-covalent dimer prototype Gal-1. The placement of the AVI-tag appears to be critical for the lectin performance as its direct attachment to the carbohydrate-binding domain of Gal-1 impaired its activity, and had to be separated with a neutral 15-amino acid linker. For Gal-1, the BLI results showed a very good agreement with the results of ITC, with K_D values in the low micromolar to nanomolar range. For Gal-3, the differences between both analytical methods were larger, with BLI showing significantly lower K_D values than ITC (low nanomolar to high picomolar range). In our experience, even large discrepancies can be observed between affinities determined by different methods, especially when comparing in-solution (ITC) and on-surface (BLI) methods [9,11]. In solution, the binding partners can freely adopt a thermodynamically stable complex where a single glycoconjugate molecule can bind several galectin molecules according to its valence. In contrast, in the surface-bound approach, a single immobilized galectin molecule interacts only with one glycan moiety of a single dendrimer at a time, i.e., with no cooperativity as reflected on the values of Hill coefficient around 1 in our BLI experiment. Moreover, the BLI experiments provide affinity constants calculated from the real time kinetics data, while the affinity constants acquired from ITC are based on steady state measurements. Hence, this may lead to the differences in the K_D values obtained from BLI and ITC measurements. In our case, this effect resulted into K_D values acquired with BLI considerably lower than those measured with ITC. Such an effect was observed previously in other lectin-ligand systems [47], so it is apparently independent of the particular structural

features of the lectin. Since the complex relationships within the interaction system are quite different in both methods, they may be very difficult, if not impossible, to fully track. In any case, no aggregation of either galectin during ITC experiments was observed, and the validity of K_D values acquired with ITC was verified using different galectin concentrations. As a result, we believe that an affinity determination by several independent methods is extremely important because it provides the closest insight into the true relation between the ligand and the lectin. Nevertheless, despite this discrepancy, the general trends observed within each galectin series were remarkably similar in both methods. Among the glycoclusters with lower valency, hexavalent cyclotriphosphazene-based **14** proved to be outstanding. This could be due to a combination of two factors, the presence of the conjugated π-electron system close to the sugar moiety as previously discussed in the literature [48], and the orientation of LacNAc ligand in the statistically most favorable arrangement for interaction. The geometry of the scaffold of glycocluster **14**, determined previously by X-ray crystallography, shows that three substituents on the phosphorous atoms are pointing upward and three are pointing downward from the planar aromatic ring [37]. In this case, this particular geometry most likely provides an appropriate distribution of the peripheral LacNAc moieties, and allows for the accommodation of several galectin monomers. In contrast, the cyclopeptide core, such as in glycocluster **12**, is structured as a β-sheet with the four functionalized lysines pointing in the same direction [49]. This geometry probably results in LacNAc moieties being displayed closer to one another, which limits the binding of several galectin monomers due to steric clashes. The higher-valent (16 to 24 LacNAc units) glycodendrimers, although still more efficient than the first-generation glycoclusters, exhibited only a slight further improvement in ligand affinity.

This study further reveals the impact of the spacer type, and the close neighborhood of the LacNAc ligand, on the binding affinity to Gal-1 and Gal-3. We conclude that the impact of the spacer (chitooligomer or triazole) is small, definitely within one order of magnitude, which was also observed previously [10,14,20,27,50]. In our own previous work [14], the positive contribution of the neighboring *N*-triazole moiety to the glycoconjugate avidity to Gal-3 was *ca* 2-fold compared to an aliphatic linker. In this study, the differences between either chitooligomer-based linker and *N*-triazole linker (*cf.* glycoconjugates **23**, and **24** to **14**) ranged between 1.5-fold to 4-fold, depending on the particular galectin and also slightly on the measurement method (BLI or ITC) – chitooligomer spacer was slightly more advantageous for Gal-1 and rather less advantageous for Gal-3 but, considering the measurement error, these results were of rather little significance.

5. Conclusion

A library of seven glycoconjugates (glycoclusters and glycodendrimers) was prepared in order to compare the binding properties of different scaffolds to Gal-1 and Gal-3. In addition, the LacNAc ligand was prepared by chemo-enzymatic synthesis on two chitooligomer spacers and conjugated to a model cyclotriphosphazene-based scaffold by copper-catalyzed azide-alkyne cycloaddition. The affinity to galectins was determined using a new set-up of biolayer interferometry with AVI-tagged constructs of galectins. The affinity results were compared with the gold-standard method of isothermal titration calorimetry and thoroughly discussed. The affinity measurements showed that the prepared compounds have a high potential for inhibition of both galectins but apparently, they are more selective for Gal-3. The K_D values for the best-performing glycoconjugates reached the low nanomolar to high picomolar range

with the BLI method. In addition, we investigated the effect of the spacer structure on the affinity to galectins, comparing a nature-like chitooligomer spacer with the heterocyclic triazole directly adjacent to the LacNAc epitope. We found the chitooligomer spacer had a slightly positive effect on binding to Gal-1 in this multivalent design whereas for Gal-3 we found no or a slightly negative effect of this spacer compared to the direct triazole linker. This may be caused by non-specific interaction of the heterocyclic triazole moiety with binding subsite E of Gal-3 as was also observed previously. Although the K_D values obtained with BLI and ITC cannot be directly compared due to extreme differences in experimental conditions and assay set-ups, it is crucial that the same trends in affinities were observed between the respective compounds, which demonstrates the complementarity of these two biophysical techniques. Due to their strong binding potency with Gal-3, the prepared glycoconjugates will be further investigated in biological assays to evaluate their effect on galectins *in vivo* and to exploit their biomedical potential.

References

[1]   F.T. Liu, G.A. Rabinovich, Galectins as modulators of tumour progression, Nat. Rev. Cancer. 5 (2005) 29–41. https://doi.org/10.1038/nrc1527.

[2]   D. Houzelstein, I.R. Gonçalves, A.J. Fadden, S.S. Sidhu, D.N.W. Cooper, K. Drickamer, H. Leffler, F. Poirier, Phylogenetic analysis of the vertebrate galectin family, Mol. Biol. Evol. 21 (2004) 1177–1187. https://doi.org/10.1093/MOLBEV/MSH082.

[3]   W. Jia, H. Kidoya, D. Yamakawa, H. Naito, N. Takakura, Galectin-3 accelerates M2 macrophage infiltration and angiogenesis in tumors, Am. J. Pathol. 182 (2013) 1821–1831. https://doi.org/10.1016/J.AJPATH.2013.01.017.

[4]   B. V. Hisrich, R.B. Young, A.M. Sansone, Z. Bowens, L.J. Green, B.A. Lessey, A. V. Blenda, Role of Human Galectins in Inflammation and Cancers Associated with Endometriosis, Biomolecules. 10 (2020). https://doi.org/10.3390/BIOM10020230.

[5]   J.M. Cousin, M.J. Cloninger, The Role of Galectin-1 in Cancer Progression, and Synthetic Multivalent Systems for the Study of Galectin-1, Int. J. Mol. Sci. 2016, Vol. 17, Page 1566. 17 (2016) 1566. https://doi.org/10.3390/IJMS17091566.

[6]   A.F. Silva-Filho, W.L.B. Sena, L.R.A. Lima, L.V.N. Carvalho, M.C. Pereira, L.G.S. Santos, R.V.C. Santos, L.B. Tavares, M.G.R. Pitta, M.J.B.M. Rêgo, Glycobiology modifications in intratumoral hypoxia: The breathless side of glycans interaction, Cell. Physiol. Biochem. 41 (2017) 1801–1829. https://doi.org/10.1159/000471912.

[7]   R.Y. Yang, G.A. Rabinovich, F.T. Liu, Galectins: Structure, function and therapeutic potential, Expert Rev. Mol. Med. 10 (2008). https://doi.org/10.1017/S1462399408000719.

[8]   N. Ahmad, H.J. Gabius, S. André, H. Kaltner, S. Sabesan, R. Roy, B. Liu, F. Macaluso, C.F. Brewer, Galectin-3 Precipitates as a Pentamer with Synthetic Multivalent Carbohydrates and Forms Heterogeneous Cross-linked Complexes, J. Biol. Chem. 279

(2004) 10841–10847. https://doi.org/10.1074/JBC.M312834200.

[9]   T. Vašíček, V. Spiwok, J. Červený, L. Petrásková, L. Bumba, D. Vrbata, H. Pelantová, V. Křen, P. Bojarová, Regioselective 3-O-Substitution of Unprotected Thiodigalactosides: Direct Route to Galectin Inhibitors, Chem. – A Eur. J. 26 (2020) 9620–9631. https://doi.org/10.1002/CHEM.202002084.

[10]   V. Heine, M. Hovorková, M. Vlachová, M. Filipová, L. Bumba, O. Janoušková, M. Hubálek, J. Cvačka, L. Petrásková, H. Pelantová, V. Křen, L. Elling, P. Bojarová, Immunoprotective neo-glycoproteins: Chemoenzymatic synthesis of multivalent glycomimetics for inhibition of cancer-related galectin-3, Eur. J. Med. Chem. 220 (2021). https://doi.org/10.1016/J.EJMECH.2021.113500.

[11]   D. Vrbata, M. Filipová, M.R. Tavares, J. Červený, M. Vlachová, M. Šírová, H. Pelantová, L. Petrásková, L. Bumba, R. Konefał, T. Etrych, V. Křen, P. Chytil, P. Bojarová, Glycopolymers Decorated with 3- O-Substituted Thiodigalactosides as Potent Multivalent Inhibitors of Galectin-3, J. Med. Chem. 65 (2022) 3866–3878. https://doi.org/10.1021/ACS.JMEDCHEM.1C01625.

[12]   M. Mammen, S.-K. Choi, G.M. Whitesides, -K Choi, Polyvalent Interactions Occur Throughout Biology Polyvalent Interactions in Biological Systems: Implications for Design and Use of Multivalent Ligands and Inhibitors**, Angew. Chem. Int. Ed. 37 (1998). https://doi.org/10.1002/(SICI)1521-3773(19981102)37:20.

[13]   J.J. Lundquist, E.J. Toone, The cluster glycoside effect, Chem. Rev. 102 (2002) 555–578. https://doi.org/10.1021/CR000418F/ASSET/CR000418F.FP.PNG_V03.

[14]   P. Bojarová, M.R. Tavares, D. Laaf, L. Bumba, L. Petrásková, R. Konefał, M. Bláhová, H. Pelantová, L. Elling, T. Etrych, P. Chytil, V. Křen, Biocompatible glyconanomaterials based on HPMA-copolymer for specific targeting of galectin-3, J. Nanobiotechnology. 16 (2018) 1–16. https://doi.org/10.1186/s12951-018-0399-1.

[15]   M.R. Tavares, M. Bláhová, L. Sedláková, L. Elling, H. Pelantová, R. Konefał, T. Etrych, V. Křen, P. Bojarová, P. Chytil, High-Affinity N-(2-Hydroxypropyl)methacrylamide Copolymers with Tailored N-Acetyllactosamine Presentation Discriminate between Galectins, Biomacromolecules. 21 (2020) 641–652. https://doi.org/10.1021/acs.biomac.9b01370.

[16]   A. Drozdová, P. Bojarová, K. Křenek, L. Weignerová, B. Henßen, L. Elling, H. Christensen, H.H. Jensen, H. Pelantová, M. Kuzma, K. Bezouška, M. Krupová, D. Adámek, K. Slámová, V. Křen, Enzymatic synthesis of dimeric glycomimetic ligands of NK cell activation receptors, Carbohydr. Res. 346 (2011) 1599–1609. https://doi.org/10.1016/J.CARRES.2011.04.043.

[17]   J.H. Ennist, H.R. Termuehlen, S.P. Bernhard, M.S. Fricke, M.J. Cloninger, Chemoenzymatic Synthesis of Galectin Binding Glycopolymers, Bioconjug. Chem. 29 (2018) 4030–4039. https://doi.org/10.1021/ACS.BIOCONJCHEM.8B00599.

[18]   I. Vrasidas, S. André, P. Valentini, C. Böck, M. Lensch, H. Kaltner, R.M.J. Liskamp, H.J. Gabius, R.J. Pieters, Rigidified multivalent lactose molecules and their interactions with mammalian galectins: a route to selective inhibitors, Org. Biomol. Chem. 1 (2003) 803–810. https://doi.org/10.1039/B210923A.

[19]   S. André, C. Grandjean, F.M. Gautier, S. Bernardi, F. Sansone, H.J. Gabius, R. Ungaro, Combining carbohydrate substitutions at bioinspired positions with multivalent presentation towards optimising lectin inhibitors: case study with calixarenes, Chem. Commun. 47 (2011) 6126–6128. https://doi.org/10.1039/C1CC11163A.

[20]   D. Laaf, P. Bojarová, B. Mikulová, H. Pelantová, V. Křen, L. Elling, Two-Step Enzymatic Synthesis of β-N-Acetylgalactosamine-(1→4)-N-acetylglucosamine (LacdiNAc) Chitooligomers for Deciphering Galectin Binding Behavior, Adv. Synth.

Catal. 359 (2017) 2101–2108. https://doi.org/10.1002/adsc.201700331.

[21] M. Hoffmann, M.R. Hayes, J. Pietruszka, L. Elling, Synthesis of the Thomsen-Friedenreich-antigen (TF-antigen) and binding of Galectin-3 to TF-antigen presenting neo-glycoproteins, Glycoconj. J. 37 (2020) 457–470. https://doi.org/10.1007/S10719-020-09926-Y/TABLES/2.

[22] A. Restuccia, Y.F. Tian, J.H. Collier, G.A. Hudalla, Self-Assembled Glycopeptide Nanofibers as Modulators of Galectin-1 Bioactivity, Cell. Mol. Bioeng. 8 (2015) 471–487. https://doi.org/10.1007/S12195-015-0399-2.

[23] A. Restuccia, M.M. Fettis, S.A. Farhadi, M.D. Molinaro, B. Kane, G.A. Hudalla, Evaluation of Self-Assembled Glycopeptide Nanofibers Modified with N, N′-Diacetyllactosamine for Selective Galectin-3 Recognition and Inhibition, ACS Biomater. Sci. Eng. 4 (2018) 3451–3459. https://doi.org/10.1021/ACSBIOMATERIALS.8B00611/SUPPL_FILE/AB8B00611_SI_001.PDF.

[24] S. Cecioni, A. Imberty, S. Vidal, Glycomimetics versus multivalent glycoconjugates for the design of high affinity lectin ligands, Chem. Rev. 115 (2015) 525–561. https://doi.org/10.1021/CR500303T/ASSET/IMAGES/CR500303T.SOCIAL.JPEG_V03.

[25] D. Goyard, B. Thomas, E. Gillon, A. Imberty, O. Renaudet, Heteroglycoclusters With Dual Nanomolar Affinities for the Lectins LecA and LecB From Pseudomonas aeruginosa, Front. Chem. 7 (2019). https://doi.org/10.3389/FCHEM.2019.00666.

[26] C. Pifferi, D. Goyard, E. Gillon, A. Imberty, O. Renaudet, Synthesis of Mannosylated Glycodendrimers and Evaluation against BC2L-A Lectin from Burkholderia Cenocepacia, Chempluschem. 82 (2017) 390–398. https://doi.org/10.1002/CPLU.201600569.

[27] L. Bumba, D. Laaf, V. Spiwok, L. Elling, V. Křen, P. Bojarová, Poly-N-acetyllactosamine Neo-glycoproteins as nanomolar ligands of human galectin-3: Binding kinetics and modeling, Int. J. Mol. Sci. 19 (2018) 1–17. https://doi.org/10.3390/ijms19020372.

[28] D.G. Gibson, L. Young, R.Y. Chuang, J.C. Venter, C.A. Hutchison, H.O. Smith, Enzymatic assembly of DNA molecules up to several hundred kilobases, Nat. Methods. 6 (2009) 343–345. https://doi.org/10.1038/NMETH.1318.

[29] M. Bradford, A Rapid and Sensitive Method for the Quantitation of Microgram Quantities of Protein Utilizing the Principle of Protein-Dye Binding, Anal. Biochem. 72 (1976) 248–254. https://doi.org/10.1006/abio.1976.9999.

[30] P. Fialová, A.T. Carmona, I. Robina, R. Ettrich, P. Sedmera, V. Přikrylová, L. Petrásková-Hušáková, V. Křen, Glycosyl azide - A novel substrate for enzymatic transglycosylations, Tetrahedron Lett. 46 (2005) 8715–8718. https://doi.org/10.1016/j.tetlet.2005.10.040.

[31] M. Hovorková, N. Kulik, D. Konvalinková, L. Petrásková, V. Křen, P. Bojarová, Mutagenesis of Catalytic Nucleophile of β-Galactosidase Retains Residual Hydrolytic Activity and Affords a Transgalactosidase, ChemCatChem. 13 (2021) 4532–4542. https://doi.org/10.1002/CCTC.202101107.

[32] P. Bojarová, N. Kulik, M. Hovorková, K. Slámová, H. Pelantová, V. Křen, The β-N-acetylhexosaminidase in the synthesis of bioactive glycans: Protein and reaction engineering, Molecules. 24 (2019) 599. https://doi.org/10.3390/molecules24030599.

[33] P. Nekvasilová, N. Kulik, N. Rychlá, H. Pelantová, L. Petrásková, Z. Bosáková, J. Cvačka, K. Slámová, V. Křen, P. Bojarová, How Site- Directed Mutagenesis Boosted Selectivity of a Promiscuous Enzyme, Adv. Synth. Catal. 362 (2020) 4138–4150. https://doi.org/10.1002/adsc.202000604.

[34] P. Nekvasilová, M. Hovorková, Z. Mészáros, L. Petrásková, H. Pelantová, V. Křen, K. Slámová, P. Bojarová, Engineered Glycosidases for the Synthesis of Analogs of Human Milk Oligosaccharides, Int. J. Mol. Sci. 23 (2022). https://doi.org/https://doi.org/ 10.3390/ijms23084106.

[35] N. Berthet, B. Thomas, I. Bossu, E. Dufour, E. Gillon, J. Garcia, N. Spinelli, A. Imberty, P. Dumy, O. Renaudet, High Affinity Glycodendrimers for the Lectin LecB from Pseudomonas aeruginosa, (2013). https://doi.org/10.1021/bc400239m.

[36] I. Bossu, N. Berthet, P. Dumy, O. Renaudet, Synthesis of Glycocyclopeptides by Click Chemistry and Inhibition Assays with Lectins, J. Carbohydr. Chem. 30 (2011) 458–468. https://doi.org/10.1080/07328303.2011.590260.

[37] L. Abbassi, Y.M. Chabre, N. Kottari, A.A. Arnold, S. André, J. Josserand, H.J. Gabius, R. Roy, Multifaceted glycodendrimers with programmable bioactivity through convergent, divergent, and accelerated approaches using polyfunctional cyclotriphosphazenes, Polym. Chem. 6 (2015) 7666–7683. https://doi.org/10.1039/C5PY01283J.

[38] P. Bojarová, P. Chytil, B. Mikulová, L. Bumba, R. Konefał, H. Pelantová, J. Krejzová, K. Slámová, L. Petrásková, L. Kotrchová, J. Cvačka, T. Etrych, V. Křen, Glycan-decorated HPMA copolymers as high-affinity lectin ligands, Polym. Chem. 8 (2017) 2647–2658. https://doi.org/10.1039/c7py00271h.

[39] E.M. Rapoport, S. André, O. V. Kurmyshkina, T. V. Pochechueva, V. V. Severov, G. V. Pazynina, H.J. Gabius, N. V. Bovin, Galectin-loaded cells as a platform for the profiling of lectin specificity by fluorescent neoglycoconjugates: A case study on galectins-1 and -3 and the impact of assay setting, Glycobiology. 18 (2008) 315–324. https://doi.org/10.1093/GLYCOB/CWN009.

[40] J. Hirabayashi, T. Hashidate, Y. Arata, N. Nishi, T. Nakamura, M. Hirashima, T. Urashima, T. Oka, M. Futai, W.E.G. Muller, F. Yagi, K.I. Kasai, Oligosaccharide specificity of galectins: A search by frontal affinity chromatography, Biochim. Biophys. Acta - Gen. Subj. 1572 (2002) 232–254. https://doi.org/10.1016/S0304-4165(02)00311-2.

[41] D. Laaf, P. Bojarová, L. Elling, V. Křen, Galectin–Carbohydrate Interactions in Biomedicine and Biotechnology, Trends Biotechnol. 37 (2019) 402–415. https://doi.org/10.1016/J.TIBTECH.2018.10.001.

[42] M. Cho, R.D. Cummings, Galectin-1: Oligomeric structure and interactions with polylactosamine, Trends Glycosci. Glycotechnol. 9 (1997) 47–56. https://doi.org/10.4052/TIGG.9.47.

[43] M. Cho, R.D. Cummings, Galectin-1, a beta-galactoside-binding lectin in Chinese hamster ovary cells. I. Physical and chemical characterization, J. Biol. Chem. 270 (1995) 5198–5206. https://doi.org/10.1074/JBC.270.10.5198.

[44] Ri-Yao Yang, Paul N. Hill, and Daniel K. Hsu, F.-T. Liu*, Role of the Carboxyl-Terminal Lectin Domain in Self-Association of Galectin-3†, Biochemistry. 37 (1998) 4086–4092. https://doi.org/10.1021/BI971409C.

[45] F.P. Schwarz, H. Ahmed, M.A. Bianchet, L.M. Amzel, G.R. Vasta, Thermodynamics of bovine spleen galectin-1 binding to disaccharides: Correlation with structure and its effect on oligomerization at the denaturation temperature, Biochemistry. 37 (1998) 5867–5877. https://doi.org/10.1021/BI9716478/ASSET/IMAGES/LARGE/BI9716478F00006.JPEG.

[46] S. Morris, N. Ahmad, S. Andre, H. Kaltner, H.J. Gabius, M. Brenowitz, F. Brewer, Quaternary solution structures of galectins-1, -3, and -7, Glycobiology. 14 (2004) 293–300. https://doi.org/10.1093/GLYCOB/CWH029.

[47] L. Picault, E. Laigre, E. Gillon, C. Tiertant, O. Renaudet, A. Imberty, D. Goyard, J. Dejeu, Characterization of the interaction of multivalent glycosylated ligands with bacterial lectins by biolayer interferometry, Glycobiology. 32 (2022) 886–896. https://doi.org/10.1093/GLYCOB/CWAC047.

[48] P. Sörme, P. Arnoux, B. Kahl-Knutsson, H. Leffler, J.M. Rini, U.J. Nilsson, Structural and thermodynamic studies on cation-II interactions in lectin-ligand complexes: High-affinity galectin-3 inhibitors through fine-tuning of an arginine-arene interaction, J. Am. Chem. Soc. 127 (2005) 1737–1743. https://doi.org/10.1021/JA043475P/SUPPL_FILE/JA043475PSI20050114_032457.PDF.

[49] I. Bossu, M. Šulc, K. Kenek, E. Dufour, J. Garcia, N. Berthet, P. Dumy, V. Křen, O. Renaudet, Dendri-RAFTs: A second generation of cyclopeptide-based glycoclusters, Org. Biomol. Chem. 9 (2011) 1948–1959. https://doi.org/10.1039/C0OB00772B.

[50] A. Restuccia, G.A. Hudalla, Tuning carbohydrate density enhances protein binding and inhibition by glycosylated β-sheet peptide nanofibers, Biomater. Sci. 6 (2018) 2327–2335. https://doi.org/10.1039/C8BM00533H.